

Basket-based Softmax

Qiang Meng¹, Xinqian Gu², Xiaqing Xu¹, Feng Zhou¹

¹Algorithm Research, Aibee Inc. ² University of Chinese Academy of Sciences

Abstract

Softmax-based losses have achieved state-of-the-art performances on various tasks such as face recognition and re-identification. However, these methods highly relied on clean datasets with global labels, which limits their usage in many real-world applications. An important reason is that merging and organizing datasets from various temporal and spatial scenarios is usually not realistic, as noisy labels can be introduced and exponential-increasing resources are required. To address this issue, we propose a novel mining-during-training strategy called *Basket-based Softmax (BBS)* as well as its parallel version to effectively train models on multiple datasets in an end-to-end fashion. Specifically, for each training sample, we simultaneously adopt similarity scores as the clue to mining negative classes from other datasets, and dynamically add them to assist the learning of discriminative features. Experimentally, we demonstrate the efficiency and superiority of the BBS on the tasks of face recognition and re-identification, with both simulated and real-world datasets.

1. Introduction

Softmax-based losses have achieved state-of-the-art performances on various tasks such as face recognition and re-identification. These methods can be classified into Euclidean margin based loss [12, 18, 26] and cosine margin (angular margin) based loss [11, 27, 3, 16]. Compared to pairwise metric learning methods such as triplet loss [20] and N-pair [22] loss, softmax-based losses have the following advantages: (a). With all negative classes in sight, models trained with softmax-based losses converge more quickly in most cases. (b). Not affected by sampling strategies and therefore have more stable training processes. (c). More discriminative features can be learned, and state-of-art performances have been witnessed on various recognition benchmarks. These characteristics are of great value in many real-world applications where training databases are of large-scale and high efficiencies are needed.

Despite the great success, softmax-based losses suffer from large GPU memory consumption as well as demand-

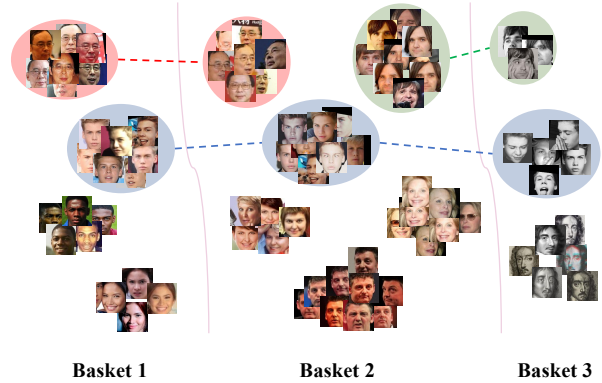


Figure 1: An illustration of the **Multiple Baskets with Class Overlaps (MBCO)** problem (simulated by faces from MS1MV2 [3]). One basket means a well-organized dataset while these baskets can be collected from different temporal/spatial scenarios or capturing conditions (e.g., images in basket 1,2 are captured with RGB cameras while basket 3 are from black-and-white cameras). Overlapped classes between baskets are indicated by dash lines.

ing clean datasets with global labels. Thanks to the development of parallel acceleration, memory assumptions can be highly decreased and that enables training on million level classes on a single machine [3]. However, a clean dataset with global labels is not always available. Instead, in many real-world applications, we may have multiple datasets captured from various temporal/spatial scenarios. Directly merging these datasets, especially for large-scale datasets, is not realistic because noisy labels can be introduced, and exponential-increasing resources are required. In this case, we call a training dataset as a basket and define the problem as **Multiple Baskets with Class Overlaps (MBCO)**, where one class is unique in a basket but can appear multiple times across baskets, as illustrated in Fig. 1. A practically significant but usually ignored question arises: how to simultaneously train softmax losses on multiple baskets with overlapped classes? We note that the raised problem is different from a well-studied problem [32, 35, 8, 29, 2] called noisy label problem, which focuses on mislabeled samples inside a class but ignore the noise of one class being assigned with

different labels. To emphasize the importance of this problem, we list a few real-world examples below:

- In surveillance scenarios, merging faces in videos captured within a small-time window is relatively easy as cues such as tracking or re-id results can be relied on. However, merging faces across days is almost impossible because of the vast volumes of the data as well as the lack of other cues.
- Merging datasets is extremely difficult when large variations exhibit. For example, face images are highly affected by image acquisition conditions (*e.g.*, illumination, background, blurriness, and low resolution) and factors of the face (*e.g.*, pose, occlusion and expression), and therefore degrades the qualities of human-assessed and similarity-based labels.
- In some situations, there lack of a clear labelling rules. For instance, whether grouping images from a same identity but with different clothes is still indistinct for person re-identification task.
- For scenarios with privacy concerns (*e.g.*, collecting faces without appropriate consents can breach the law), pipelines which can automatically collect data, train and deploy models are preferred. Automatically generating small and clean datasets is relatively easy. However, noise will be accumulated in absence of manual interventions with the increasing of data volumes. Consequently, models trained on such noisy datasets will encounter performance degradations. In this case, models are better trained on multiple clean baskets, instead of a large but noisy dataset.

To enable training on multiple baskets with softmax-based losses, we propose a framework called Basket-based Softmax (BBS) which works in an end-to-end fashion and can be applied to most softmax-based losses. Specifically, we simultaneously use the similarity scores defined in softmax losses as the clue to mining negative classes from other baskets, and dynamically add them to guide the learning of more discriminative features. To better fit the large-scale issue in practical applications, we further modified the BBS to the parallel version. Extensive experiments are conducted to verify the superiority and efficiency of our proposed method. We summarize our contributions as follows:

1. We raise the importance of the Multiple Baskets with Class Overlaps (MBCO) problem which is usually ignored by the academic community but can occur frequently in many real-world applications. Datasets collected from various temporal and spatial scenarios can be of tremendous size and labels are locally assigned in each basket. Directly assigning global classes

can introduce noisy labels and requires exponential-increasing resources.

2. An efficient and end-to-end mining-during-training framework called BBS is proposed, where similarity scores are adopted as the cue to dynamically mining negative classes across baskets. Our proposed BBS can be applied to the majority softmax-based losses and trained on multiple baskets simultaneously. Besides that, we also introduce the parallel version to enable the training of million level classes.
3. Experimentally, we modified the common-used Softmax, CosFace [27] and ArcFace [3] to our BBS framework. Extensive experiments are conducted on face recognition and person re-identification and verify the superiority of BBS, with both simulated and real-world training datasets.

2. Related Works

2.1. Deep Face Recognition

Recent years have witnessed the breakthrough of deep convolutional face recognition techniques [11, 27, 3, 33, 14, 16, 15]. Most of early works rely on metric-learning based loss, including contrastive loss [1], triplet loss [20], n-pair loss [22], angular loss [28], *etc.* Suffering from the combinatorial explosion in the number of face triplets, embedding-based method is usually inefficient in training on large-scale dataset. Therefore, the main body of research in deep face recognition has focused on devising more efficient and effective softmax-based loss. Wen *et al.* [30] develop a center loss to learn centers for each identity to enhance the intra-class compactness. L_2 -softmax [18] and NormFace [26] study the necessity of the normalization operation and applied L_2 normalization constraint on both features and weights.

From then on, several angular margin-based losses and progressively improve the performance on various benchmarks to the newer level. SphereFace [11] introduced angular margin to softmax loss and achieved discriminative features. To overcome the optimization difficulty of SphereFace, CosFace [27] moves the angular margin into cosine space. In ArcFace [3], decision boundary is directly maximized in angular (arc) space based on the normalized weights and features, and they achieve state-of-the-art performances on current benchmarks.

2.2. Person Re-identification

Person re-identification (re-id) aims to retrieval the images of the target person from the gallery set across different cameras. The widely used losses for CNN-based re-id methods include two types: classification loss [24] and metric learning loss [6]. Classification loss views re-id

Method	Softmax	L-Softmax [12]	l_2 -softmax [18]	NormFace [26]	SphereFace [11]	CosFace [27]	ArcFace [3]
bias	✓	✗	✓	✗	✗	✗	✗
s	✗	✗	✓	✓	✗	✓	✓
$f(W, x)$	$W^T x$	$\ W\ \ x\ \psi(\theta)$	$\ W\ \cos(\theta)$	$\cos(\theta)$	$\ x\ \psi(\theta)$	$\cos(\theta) - m$	$\cos(\theta + m)$
$g(W, x)$	$W^T x$	$\ W\ \ x\ \cos(\theta)$	$\ W\ \cos(\theta)$	$\cos(\theta)$	$\ x\ \cos(\theta)$	$\cos(\theta)$	$\cos(\theta)$

Table 1: A unified perspective of softmax-based losses. Here $\theta = \frac{W^T x}{\|W\| \|x\|}$ and the ✓/✗ denotes used or not in the corresponding work. For L-softmax and SphereFace, the function ψ is defined as $\psi(\theta) = (-1)^k \cos(m\theta) - 2k$, $\theta \in [\frac{k\pi}{m}, \frac{(k+1)\pi}{m}]$, $k \in [0, m-1]$, $m \geq 1$.

in the training stage as a classification task and uses softmax with cross entropy loss to optimize the model. Sun *et al.* [23] demonstrate that other softmax-based losses, which are widely used in face recognition *e.g.*, AM-Softmax [25], CircleLoss [23], are also suitable for re-id. The most well-known metric learning loss for re-id is triplet loss with hard sample mining [6]. For each anchor in a mini-batch, triplet loss with hard sample mining only samples its hardest positive sample and its hardest negative sample to form a triplet to optimize. To take all samples to participate in optimization, Ristani *et al.* [19] improve it by proposing an adaptive weighted triplet loss and a new technique for hard-identity mining.

2.3. Noisy Labels

Learning with noisy labels has recently drawn much attention as ambiguous and inaccurate labels can exist in most datasets. Wu *et al.* [32] proposes a semantic bootstrapping method by re-labelling noisy samples by predictions. Zhong *et al.* [35] learns discriminative face representation supervised by a noise-resistant loss and copes the long-tail issue by hard identities mining strategy. Hu *et al.* [8] discovers the distribution of training samples implicitly reflects the probability to be clean and proposes a noise-tolerant end-to-end paradigm by employing the idea of weighting training samples. Co-Mining [29] trains twin networks simultaneously, detects noisy labels based on loss values, exchanges high confidence clean faces and re-weight the predicted clean faces. To improve the robustness to label noise of ArcFace, Sub-center ArcFace [2] relaxes the intra-class constraint by designing K sub-centers for each class and one training sample only needs to be close to any of the K positive sub-centers instead of the only one positive center. These methods mainly deal with the purity issue which means one class may contain multiple identities. In contrast, our BBS focuses on training the multiple baskets with class overlaps.

3. Methodology

Our goal is to learn discriminative features from multiple baskets with softmax-based losses, wherein labels inside a basket are clean while class overlaps can exist be-

tween baskets. To achieve this goal, we propose a novel mining-during-training strategy called Basket-based Softmax (BBS) to effectively train models on multiple baskets in an end-to-end fashion. We first provide a unified perspective for softmax-based losses in Sec. 3.1 and present the details of our BBS in Sec. 3.2.

In real-world applications, dealing with large-scale datasets is another non-negligible problem. To address this, we modified the original BBS to a parallel version in Sec. 3.3, which enables BBS to support million level classes on a single machine.

3.1. A Unified Perspective of Softmax-based loss

Assuming there are n classes in the training dataset and the feature embedding is of dimension d . The softmax-based losses build a fully connected layer with a weight matrix $[W_1, W_2, \dots, W_n] \in \mathcal{R}^{d \times n}$ and biases $[b_1, b_2, \dots, b_n] \in \mathcal{R}^n$, where each W_i corresponds to the class center i . For the sample i , denote its class as y_i and the embedding as x_i . The softmax-based losses for sample i can be unified into one formula as follows:

$$L = -\log \frac{e^{s(f(W_{y_i}, x_i) + b_{y_i})}}{e^{s(f(W_{y_i}, x_i) + b_{y_i})} + \sum_{j=1, j \neq y_i}^n e^{s(g(W_j, x_i) + b_j)}} \quad (1)$$

In different methods, $f(W, x), g(W, x)$ are defined in various formats as shown in Tab. 1. The function $g(W, x)$ is used to measure similarity between feature x and class center W . Softmax and L-Softmax [12] uses the Euclidean distance while NormFace [26], CosFace [27] and ArcFace [3] uses the cosine similarity. l_2 -softmax [18] and SphereFace [11] modify the similarities to eliminate the effects of magnitudes of features or class centers.

$f(W, x)$ is either the same as $g(W, x)$, or revised to further increase the intra-class distance as well as decrease inter-class distance (*e.g.*, an additive angular margin is introduced in ArcFace [3]).

3.2. Basket-based Softmax

Assuming there are M training baskets S_1, S_2, \dots, S_M and basket S_m contains N_m classes, $m = 1, 2, \dots, M$. The local class in basket m starts from 1 to N_m and we sequen-

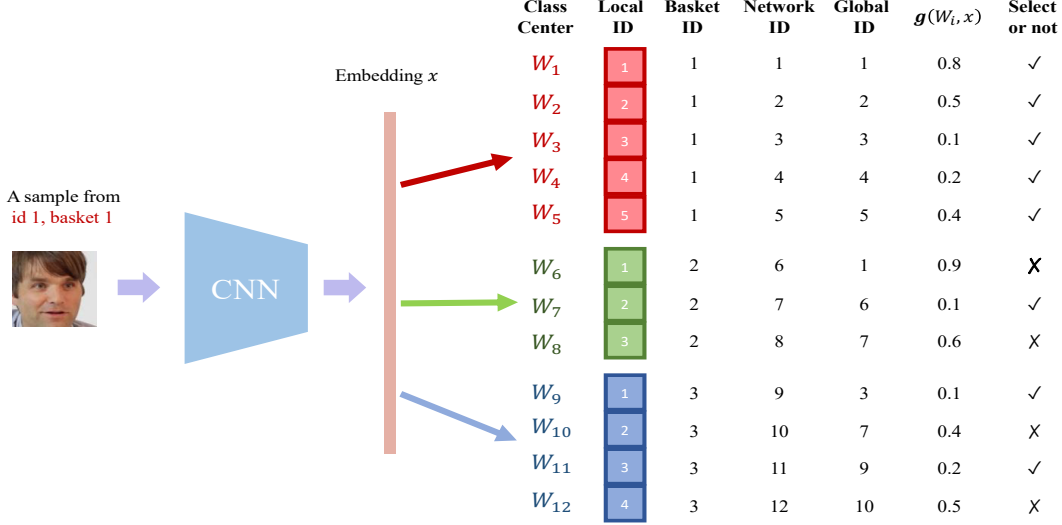


Figure 2: An example for the proposed Basket-based Softmax (BBS) with mining $N_k - 2$ negative samples, where N_k is the number of classes in the basket k . In this example, there are 3 baskets with 5, 3, 4 classes respectively. Local IDs are concatenated based on basket IDs and form the Network IDs. Global IDs indicate the real class (e.g., images with same global id in face recognition means they are collected from the same person.) In this example, class 2 in basket 2 and classes 1,3 in basket 3 are added to negative classes for current sample.

tially concatenate labels from all baskets to get the network labels, as shown in Fig. 2.

Denote $L_0 = 0, L_m = \sum_{i=1}^{m-1} N_i, m = 1, 2, \dots, M$. Then the total number of network ids is L_M . For the sample x_i with basket id m and local id l , its network id is $L_{m-1} + l$ in our setting. For the sake of expression, we define the following functions:

$$\begin{aligned} F(m, l, x_i) &= e^{s(f(W_{L_{m-1}+l}, x_i) + b_{L_{m-1}+l})} \\ G(m, l, x_i) &= e^{s(g(W_{L_{m-1}+l}, x_i) + b_{L_{m-1}+l})} \end{aligned} \quad (2)$$

Then the loss for basket-based softmax is formulated as follows:

$$L_{bbs} = -\log \frac{F(m, l, x_i)}{F(m, l, x_i) + \sum_{\substack{j=1 \\ j \neq l}}^{N_m} G(m, j, x_i) + \sum_{\substack{k=1 \\ k \neq m}}^M \sum_{j=1}^{N_k} G(k, j, x_i) \cdot p_{(L_k+j)}^i} \quad (3)$$

Here $p_{(L_k+j)}^i \in (0, 1)$ is an indicator whether adding class j in basket k as a negative class for current sample i . When $p_{(L_k+j)}^i = 0$ for all k, j , each basket is assigned with an individual loss and BBS loss degrades to the multi-task approach (e.g., each basket has an individual loss). In contrast, setting all $p_{(L_k+j)}^i$ to 1 has the same effect of training on concatenated data, without considering the overlapped classes between baskets.

Function $g(W, x)$ is used as a metric for measuring the similarity between an embedding x and a class center W . For each sample i from basket m , we select n_k negative classes from basket k ($k = 1, 2, \dots, N_k, k \neq m$) based on the similarities. To be more specific, similarities of current

embedding and class centers of basket k are calculated and n_k least similar class centers are picked as negative classes. We summarize the training scheme in Algorithm 1.

Algorithm 1: Basket-based Softmax

- 1 **Input:** Training sets $S_m, m = 1, 2, \dots, M$ with N_m identities and the mining number n_m .
 - 2 **while** NOT end of training **do**
 - 3 Update training parameters such as learning rate and weight decay, etc. ;
 - 4 Take sample i with basket id m and extract its embedding x_i ;
 - 5 Initialize a L_M -length array p^i with 1s;
 - 6 **for** $k = 1, 2, \dots, M, k \neq m$ **do**
 - 7 **for** $j = 1, 2, \dots, N_k$ **do**
 - 8 $v_j \leftarrow g(W_{(L_k+j)}, x_i)$;
 - 9 $v = [v_1, v_2, \dots, v_{N_k}]$;
 - 10 **for** $j = 1, 2, \dots, N_k$ **do**
 - 11 **if** v_j among top- d_k of v **then**
 - 12 $p_{(L_k+j)}^i = 0$
 - 13 Calculate BBS loss of current data i based on Eq. (3) and update model parameters by back-propagation;
-

3.2.1 Dynamic Negative Class Mining

A hyperparameter of our BBS is the number of negative class centers n_k from basket k . In the ideal situation, n_k can be set to be $N_k - 1$ as current sample i belongs to at most one class in that basket. However, this hyperparameter highly relies on the qualities of estimated similarities. If model is not discriminative enough, a smaller n_k should be used. To this end, we design a dynamic mining strategy as shown in Algorithm. 2.

We define $d_k = N_k - n_k$ as the number of ignored classes in basket k , which indicates that we cannot treat top- d_k similar classes to be negative classes with a high confidence. We set a minimum ignored number $\tau_k, \tau_k \geq 1$ and an ignored ratio r_k . The r_k is dynamically adjusted based on the discriminative ability of the model. Its value is monotonically decreased during our training process. In the end, we have $d_k = \max(\tau_k, N_k \cdot r_k)$.

Algorithm 2: Dynamic mining during training

- 1 **Input:** Minimum ignored number τ_k , the ignored ratio r_k dropped every t_r epochs and M baskets of training sets S_1, S_2, \dots, S_M . Training total T epochs.
 - 2 **for** $t = 1, 2, \dots, T$ **do**
 - 3 **for** $k = 1, 2, \dots, M$ **do**
 - 4 $r_k = \lceil \frac{T-t}{t_r} \rceil \cdot \frac{t_r}{T}$;
 - 5 Update $n_k = N_k - \max(\tau_k, N_k \cdot r_k)$;
-

3.3. Parallel Basket-based Softmax

For the parallel version of BBS, we first distribute L_M class centers into G GPUs with $W_{l_g}, W_{l_g+1}, \dots, W_{u_g}$ assigned to the g -th GPU, where $l_g = g \cdot \lceil \frac{L_M}{G} \rceil$ and $u_g = \min((g+1) * \lceil \frac{L_M}{G} \rceil - 1, L_M)$. For a sample i from basket m and with the network id y_i , we have the following parallel BBS:

$$L_{pbbS} = -\log \frac{e^{s(f(W_{y_i}, x_i) + b_{y_i})}}{e^{s(f(W_{y_i}, x_i) + b_{y_i})} + \sum_{g=1}^G \sum_{j=l_g}^{u_g} p_j^i \cdot e^{s(g(W_j, x_i) + b_j)}} \quad (4)$$

Here $p_j^i \in \{0, 1\}$. For classes belongs to basket m , then we set p_j^i to be 0 if $j = y_i$ and 1 otherwise. The remaining question is how to decide values for classes not in basket m .

Because of being distributed, class centers belong to one basket may distribute to multiple GPUs. Consequently, one GPU has no access to all similarities without gathering the scores together. To avoid extra GPU memories consumption, we propose the algorithm 3 to approximate procedure in lines 6-13 in algorithm 1. For example, x_i with basket ID m , the key idea of the parallel version is to consider each

truncated basket as a new one and calculate the number of negative classes based on the new baskets.

Algorithm 3: Setting p for Parallel BBS

- 1 Initialize a L_M -length array p^i with all elements set to 1 besides $p_{y_i}^i \leftarrow 0$;
 - 2 **for each GPU** g **do**
 - 3 **for** $k = 1, 2, \dots, M, k \neq m$ **do**
 - 4 $l \leftarrow \max(0, L_{m-1} - g_l)$;
 - 5 $u \leftarrow \min(N_G, L_m - g_u)$;
 - 6 **if** $l \geq N_G$ **or** $u \neq 0$ **then**
 - 7 **continue** ;
 - 8 **for** $j = l, l+1, \dots, u$ **do**
 - 9 $v_j \leftarrow -g(W_{g_l+j}, x_i)$;
 - 10 $v = [v_l, v_{l+1}, \dots, v_u]$;
 - 11 $d_k^g = \max(\tau_k, (u-l+1) \cdot r_k)$;
 - 12 **for** $j = l, l+1, \dots, u$ **do**
 - 13 **if** v_j **is among top-** d_k^g **of** v **then**
 - 14 $p_{l_g+j}^i = 0$;
 - 15 Calculate $p_j^i \cdot e^{s(g(W_j, x_i) + b_j)}$ in each GPU and Gather the results ;
 - 16 Compute the L_{pbbS} according to Eq. 4;
-

4. Experiment

We evaluate our BBS on two important tasks in the computer vision community: face recognition (section 4.1) and person re-identification (section 4.2). For face recognition, we simulate the MBCO problem for experiments on a common-used database called MS1MV2 [3]. For person re-identification, images from same camera and in same day are gathered to be a basket. As lack of previous works on this problem, we choose two baselines: the first baseline is trained on the concatenated baskets without merging classes, while the second baseline is the multi-task approach with each basket equipped with a softmax loss. To further verify the capability of handling large-scale data, resource consumptions are studied when modifying BBS to the parallel version (in section 4.3).

4.1. Face Recognition

To simulate the MBCO problem, we adopt the algorithm 4 to split a dataset D into k baskets, where one class appears in l baskets with the probability p_l . We modify the state-of-the-art ArcFace [3] in face recognition to our BBS framework and conduct experiments by our simulated baskets. We mainly consider two important factors of the MBCO problem: ratio of class overlaps between baskets (in section 4.1.2) and number of baskets involved (in section 4.1.3).

Algorithm 4: Split a dataset

- 1 **Input:** A dataset D . Number of parts k and the probability array $p = [p_1, p_2, \dots, p_k]$.
 - 2 **for** each label in D **do**
 - 3 Sample a number l from $[1, 2, \dots, k]$ with probability p_l ;
 - 4 Split images of current label into l parts, denote as s_1, s_2, \dots, s_l ;
 - 5 Select l datasets from D_1, D_2, \dots, D_k and insert image sets s_1, s_2, \dots, s_l orderly;
 - 6 **Output:** D_1, D_2, \dots, D_k .
-

4.1.1 Settings

Datasets. The MS-Celeb-1M dataset [4] contains about 100k identities with 10 million images. However, it consists of a great many noisy face images. We employ MS1MV2 [3] (3.8M images, 85k unique identities) as our training dataset. For evaluation, we adopt LFW [9], CFP-FP [21], AgeDB-30 [17], IJB-B [31] and IJB-C [13]. All the images are aligned to 112×112 based on 5 facial landmarks, following ArcFace [3].

Simulated Datasets. In section 4.1.2, we split the full MS1MV2 dataset into 2 parts with different ratios of class overlaps, from 10% to 100%. In section 4.1.3, MS1MV2 is split into 10 parts with $p_i = 3p_{i+1}$ (e.g., the probability of a class appears i baskets is 3 times of it appears in $i + 1$ baskets). In the end, we have $p_i = \frac{2}{3^{10-i}} \cdot 3^{(10-i)}$ and the average ratio of overlaps between two baskets is around 10%. The average number of classes in one basket is 12810.9 and experiments are conducted from 2 to 10 baskets to examine the impact of basket numbers.

Training. We train the models with 8 1080Ti GPUs by stochastic gradient descent (SGD) algorithm. The learning rate is initialized as 0.1 and divided by 10 at 5, 10, 15 epochs, and we finish the training at the 20th epoch. The weight decay is set to 0.0005 and the momentum is 0.9. We only augment the training samples by random horizontal flip. Because of vast number of identities, the parallel BBS is adopted in the face recognition experiments.

4.1.2 Ratio of Class Overlaps between Baskets

Results with different ratios of class overlaps are listed in Tab. 2. When the ratio equals to 10%, BBS surpasses the best results of two baselines by 0.08%, 0.03%, 0.03% on LFW, CFP-FP and AgeDB. The numbers are 1.57%, -0.02% , 0.20% on IJB-B at TAR@FAR=1e-5, 1e-4, 1e-3 and 0.52%, -0.05% , 0.15% on IJB-C at TAR@FAR=1e-5, 1e-4, 1e-3. When the ratio of overlaps increases, BBS has stable high

performances while the performances of two baselines drop rapidly. Taking the ratio of 100% as an example, BBS surpasses the best results of two baselines by 0.54%, 3.56%, 6.29% on LFW, CFP-FP and AgeDB. The numbers are 20.60%, 17.21%, 14.00% on IJB-B at TAR@FAR=1e-5, 1e-4, 1e-3 and 18.01%, 15.57%, 12.43% on IJB-C at TAR@FAR=1e-5, 1e-4, 1e-3.

We further visualize the trend of performances on IJB-C at TAR@FAR=1e-4 in Fig. 3. With increasing ratio of class overlaps, performance of the baseline1 drops rapidly as the error of labels increases. Labels used by baseline2 are clean as each basket are processed individually. However, with more images separated into different baskets, each class contains less images and that leads to the performance degrade. In contrast, our BBS achieves the stable and best results on TAR@FAR=1e-4 at IJB-C, which shows the superiority of the proposed method compared to the baselines.

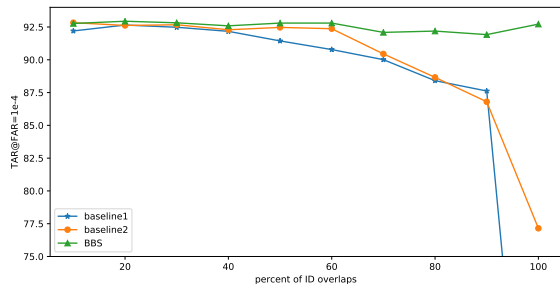


Figure 3: TAR@FAR=1e-4 on IJB-C dataset with different overlaps. With increasing ratios of overlaps, performances of two baselines drop significantly especially with ratio larger than 60%. In contrast, BBS achieves consistent the best results.

4.1.3 Number of Baskets

Tab. 3 shows the results with different number of baskets. The overall trend is that improvements become more significant with more baskets used. When all baskets used, BBS gets 0.14%, 0.33%, 0.48% performance boosts compared to the best results from baselines on LFW, CFP-FP and AgeDB. BBS also surpasses the baselines on all TAR criteria by 1.58% on FAR=1e-5, 0.81% on FAR=1e-4 and 0.56% on FAR=1e-3 than the best results from baselines on IJB-B and by 0.56% on FAR=1e-5, 0.34% on FAR=1e-4 and 0.29% on FAR=1e-3 than best results from baselines on IJB-C. We also train the model with the original MS1MV2 and report the results in the last row of table 3. Even trained with the split datasets, our BBS can still obtain comparable results to the full clean data, which demonstrates the great practical value and efficiency of the proposed method.

Split MS1MV2 into	Method	LFW	CFP-FP	AgeDB	IJB-B (TAR@FAR)			IJB-C (TAR@FAR)		
					1e-5	1e-4	1e-3	1e-5	1e-4	1e-3
2 baskets, overlap 10%	baseline1	99.63	93.48	97.10	78.96	90.04	94.03	86.10	92.20	95.45
	baseline2	99.56	93.57	97.05	82.66	90.70	94.04	88.48	92.83	95.51
	BBS	99.68	93.70	97.13	84.23	90.68	94.24	89.00	92.77	95.66
2 baskets, overlap 20%	baseline1	99.58	93.14	96.75	83.33	90.29	94.01	88.77	92.65	97.41
	baseline2	99.50	93.20	97.08	82.26	90.61	94.07	88.20	92.62	95.47
	BBS	99.67	93.67	97.15	83.80	91.02	94.02	89.18	92.94	97.42
2 baskets, overlap 30%	baseline1	99.60	92.64	96.81	82.24	90.19	93.69	87.86	92.48	95.14
	baseline2	99.52	93.31	96.88	82.02	90.48	94.28	88.06	92.67	95.42
	BBS	99.58	93.47	97.23	81.65	90.91	94.03	88.07	92.82	95.46
2 baskets, overlap 40%	baseline1	99.58	93.20	96.80	81.89	89.66	93.66	87.77	92.17	95.13
	baseline2	99.52	93.10	97.01	80.24	90.05	94.09	87.32	92.29	95.47
	BBS	99.62	93.73	96.98	80.59	90.60	94.42	87.18	92.59	95.65
2 baskets, overlap 50%	baseline1	99.63	92.35	96.36	80.98	88.94	93.12	87.07	91.44	94.73
	baseline2	99.55	93.14	97.00	81.77	90.34	94.13	88.11	92.47	95.50
	BBS	99.68	93.14	97.30	81.41	90.56	94.35	88.37	92.80	95.65
2 baskets, overlap 60%	baseline1	99.53	92.18	96.08	81.11	88.49	92.67	86.42	90.78	94.32
	baseline2	99.65	93.07	97.03	78.74	89.95	93.97	86.76	92.37	95.45
	BBS	99.70	93.47	97.13	81.28	90.63	94.28	88.33	92.80	95.57
2 baskets, overlap 70%	baseline1	99.57	92.45	95.60	79.15	87.40	92.44	84.54	90.01	94.16
	baseline2	99.65	92.40	96.76	71.01	87.71	93.47	81.96	90.45	94.94
	BBS	99.72	93.43	96.90	78.70	89.82	93.98	86.25	92.09	95.36
2 baskets, overlap 80%	baseline1	99.50	91.48	94.46	73.68	85.29	91.24	81.99	88.41	93.22
	baseline2	99.57	91.70	96.93	75.48	85.86	92.30	81.17	88.66	93.86
	BBS	99.65	93.21	97.05	81.30	89.75	94.05	86.95	92.19	95.44
2 baskets, overlap 90%	baseline1	99.50	90.40	93.81	73.38	84.32	90.72	80.09	87.62	92.92
	baseline2	99.32	89.22	92.30	74.11	83.60	89.14	79.87	86.80	91.51
	BBS	99.67	93.56	96.87	79.75	89.71	94.04	85.84	91.92	95.39
2 baskets, overlap 100%	baseline1	99.03	89.95	90.63	17.18	37.57	75.00	23.85	46.31	83.21
	baseline2	97.87	84.85	80.06	63.76	73.23	80.25	70.49	77.15	82.99
	BBS	99.57	93.41	96.92	83.37	90.44	94.25	88.50	92.72	95.64

Table 2: Verification accuracy (%) on LFW, CFP-FP, AgeDB-30 and IJB-B/IJB-C. Backbone: ResNet18.

Datasets	Method	LFW	CFP-FP	AgeDB	IJB-B (TAR@FAR)			IJB-C (TAR@FAR)		
					1e-5	1e-4	1e-3	1e-5	1e-4	1e-3
2 baskets	baseline1	99.45	88.80	95.30	78.46	86.32	91.57	83.78	89.01	93.49
	baseline2	99.38	89.00	95.45	74.26	86.38	91.71	83.02	89.11	93.51
	BBS	99.43	89.70	95.51	77.16	86.49	91.88	83.68	89.14	93.57
4 baskets	baseline1	99.38	90.46	96.11	81.64	88.50	92.94	86.97	91.22	94.49
	baseline2	99.55	91.21	96.08	79.70	88.63	93.01	86.82	91.23	94.67
	BBS	99.60	91.63	96.37	80.84	88.79	93.17	86.50	91.42	94.71
6 baskets	baseline1	99.47	91.50	96.30	82.06	88.97	93.05	86.89	91.39	94.56
	baseline2	99.45	92.56	96.42	79.32	89.49	93.37	86.38	91.83	94.98
	BBS	99.60	92.57	96.72	82.42	89.31	93.67	86.95	91.77	95.12
8 baskets	baseline1	99.38	92.63	96.52	80.80	88.72	93.11	86.81	91.20	94.71
	baseline2	99.63	93.20	96.50	80.05	89.80	93.65	86.78	91.93	95.12
	BBS	99.72	93.51	96.67	81.19	90.01	93.81	87.60	92.16	95.23
10 baskets	baseline1	99.43	92.41	96.52	80.45	89.61	93.27	87.35	91.79	94.87
	baseline2	99.53	93.51	96.65	78.95	89.90	93.85	86.74	92.31	95.34
	BBS	99.67	93.84	97.03	82.03	90.71	94.29	87.91	92.65	95.63
MS1MV2	ArcFace	99.62	93.20	96.82	83.83	91.13	94.22	89.44	93.20	95.57

Table 3: Verification accuracy (%) on LFW, CFP-FP, AgeDB-30 and IJB-B/IJB-C. Backbone: ResNet18.

4.2. Person Re-identification

In this section, we verify the generalization of our proposed BBS on person re-identification. Specifically, three losses, including Softmax with cross entropy loss, Cos-

Face [27] loss, and ArcFace [3] loss, are used as the training loss respectively to verify the generalization of the proposed BBS.

Loss	Method	top-1	top-5	mAP
Softmax	baseline1	85.4	94.2	65.9
	baseline2	78.4	89.9	53.9
	BBS	86.0	94.7	67.8
CosFace [27]	baseline1	89.0	85.9	73.6
	baseline2	85.3	93.2	64.0
	BBS	90.8	96.4	76.6
Arcface [3]	baseline1	88.5	96.0	72.7
	baseline2	84.9	91.8	63.4
	BBS	89.7	96.3	75.9

Table 4: The results with different losses on Market-Basket.

4.2.1 Settings

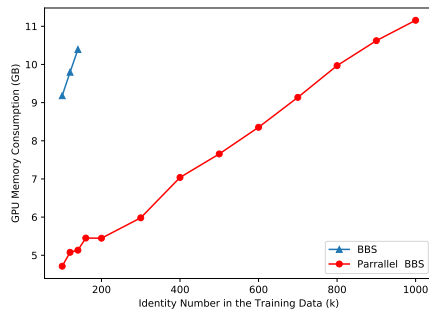
Dataset Market-1501 dataset [34] contains 1501 identities and 32217 images captured by 6 cameras. Following [34], 751 identities are reserved for training and the remaining 750 identities are used for testing. All these data are captured from six time periods. To verify the effectiveness of the proposed BBS, we divide the training set of Market-1501 into six baskets according to the capture time and name it Market-Basket dataset. In the testing stage, we use the original testing set of Market-1501 as the testing set of Market-Basket for evaluation.

Implementation Details. Following [7], We use ResNet-50 [5] as the backbone. The model is trained for 60 epochs in total by Adam [10] optimizer. The learning rate is initialized as 3.5×10^{-4} and multiplied by 0.1 after every 20 epochs. The batch size is set to 64, and each batch consists of 16 persons and 4 images for each person. All these images are resized to 256×128 pixels. We also use horizontal flip, random crop, and random erase [36] for data augmentation. As for CosFace loss and ArcFace loss, the scaling factor s is set to 16 and the margin m is set to 0.1 by grid search. For BBS, (τ_k, t_r) are set to (2,2), respectively.

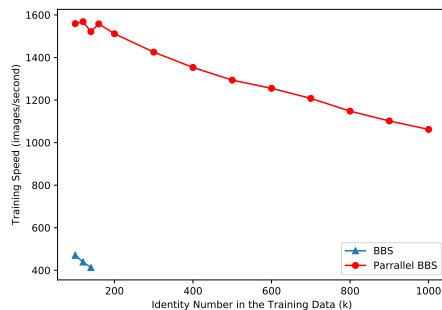
Evaluation Protocol. Cumulative Matching Characteristics (CMC) and mean Average Precision (mAP) are used as the evaluation metrics.

4.2.2 Generalization for Different Losses

As shown in Table 4, BBS surpasses baseline1 and baseline2 significantly and consistently for all these three losses. Specifically, BBS increases about 2% top-1 and 3% mAP over baseline1 for CosFace, which does not mine any cross-basket negative class. This comparison demonstrates the effectiveness of BBS for dynamic negative class mining and the generalization of BBS for different softmax-based losses.



(a) GPU Memory



(b) Training Speed

Figure 4: Parallel acceleration. Setting: ResNet 18, batch size 512, feature dimension 512, 8 GPU 1080Ti (12GB).

4.3. Parallel Acceleration

We simulate the trainings on different number of classes on 8 GPUs (1080Ti with 12GB memory) to test the training speed of the BBS and parallel BBS and visualize the results in Fig. 4. The original BBS can train less than 200k classes and the throughputs are smaller than 500 images per second. In contrast, the parallel BBS is able to handle datasets with up to 1M classes and the throughputs can be 3 times those of the original BBS. The throughputs remain more than 1000 images per second even trained with 1M classes.

5. Conclusion

In this paper, we raise the importance of the Multiple Baskets with Class Overlaps (MBCO) problem which is usually ignored by the academic community but can occur frequently in real-world applications, and propose an end-to-end mining-during-training framework called Basket-based Softmax (BBS) to enable the training on multiple baskets. Extensive experiments are conducted on face recognition and person re-identification, and have verified the superiority, efficiency as well as the generalization of our proposed method.

References

- [1] Sumit Chopra, Raia Hadsell, and Yann LeCun. Learning a similarity metric discriminatively, with application to face verification. In *IEEE Conf. Comput. Vis. Pattern Recog.*, volume 1, pages 539–546. IEEE, 2005. 2
- [2] Jiankang Deng, Jia Guo, Tongliang Liu, Mingming Gong, and Stefanos Zafeiriou. Sub-center arcface: Boosting face recognition by large-scale noisy web faces. In *Eur. Conf. Comput. Vis.*, 2020. 1, 3
- [3] Jiankang Deng, Jia Guo, Niannan Xue, and Stefanos Zafeiriou. ArcFace: Additive angular margin loss for deep face recognition. In *IEEE Conf. Comput. Vis. Pattern Recog.*, pages 4690–4699, 2019. 1, 2, 3, 5, 6, 7, 8
- [4] Yandong Guo, Lei Zhang, Yuxiao Hu, Xiaodong He, and Jianfeng Gao. MS-Celeb-1M: A dataset and benchmark for large-scale face recognition. In *European conference on computer vision*, pages 87–102. Springer, 2016. 6
- [5] Kaifeng He, Xiangyu Zhang, Shaoqing Ren, and Jian Sun. Deep residual learning for image recognition. In *IEEE Conf. Comput. Vis. Pattern Recog.*, 2016. 8
- [6] Alexander Hermans, Lucas Beyer, and Bastian Leibe. In defense of the triplet loss for person re-identification. *ArXiv:1703.07737*, 2017. 2, 3
- [7] Ruibing Hou, Bingpeng Ma, Hong Chang, Xinqian Gu, Shiguang Shan, and Xilin Chen. Interaction-and-aggregation network for person re-identification. In *IEEE Conf. Comput. Vis. Pattern Recog.*, 2019. 8
- [8] Wei Hu, Yangyu Huang, Fan Zhang, and Ruirui Li. Noise-tolerant paradigm for training face recognition cnns. In *IEEE Conf. Comput. Vis. Pattern Recog.*, pages 11887–11896, 2019. 1, 3
- [9] Gary B Huang, Marwan Mattar, Tamara Berg, and Eric Learned-Miller. Labeled faces in the wild: A database for studying face recognition in unconstrained environments. 2008. 6
- [10] Diederik P Kingma and Jimmy Ba. Adam: A method for stochastic optimization. In *Int. Conf. Learn. Represent.*, 2015. 8
- [11] Weiyang Liu, Yandong Wen, Zhiding Yu, Ming Li, Bhiksha Raj, and Le Song. SpheroFace: Deep hypersphere embedding for face recognition. In *IEEE Conf. Comput. Vis. Pattern Recog.*, pages 212–220, 2017. 1, 2, 3
- [12] Weiyang Liu, Yandong Wen, Zhiding Yu, and Meng Yang. Large-margin softmax loss for convolutional neural networks. In *ICML*, page 7, 2016. 1, 3
- [13] Brianna Maze, Jocelyn Adams, James A Duncan, Nathan Kalka, Tim Miller, Charles Otto, Anil K Jain, W Tyler Niggel, Janet Anderson, Jordan Cheney, et al. Iarpa janus benchmark-c: Face dataset and protocol. In *International Conference on Biometrics (ICB)*, pages 158–165. IEEE, 2018. 6
- [14] Qiang Meng, Xiaoqing Xu, Xiaobo Wang, Yang Qian, Yunxiao Qin, Zezheng Wang, Chenxu Zhao, Feng Zhou, and Zhen Lei. Poseface: Pose-invariant features and pose-adaptive loss for face recognition. *arXiv preprint arXiv:2107.11721*, 2021. 2
- [15] Qiang Meng, Chixiang Zhang, Xiaoqiang Xu, and Feng Zhou. Learning compatible embeddings. In *Int. Conf. Comput. Vis.*, 2021. 2
- [16] Qiang Meng, Shichao Zhao, Zhida Huang, and Feng Zhou. MagFace: A universal representation for face recognition and quality assessment. In *IEEE Conf. Comput. Vis. Pattern Recog.*, 2021. 1, 2
- [17] Stylianos Moschoglou, Athanasios Papaioannou, Christos Sagonas, Jiankang Deng, Irene Kotsia, and Stefanos Zafeiriou. Agedb: the first manually collected, in-the-wild age database. In *IEEE Conf. Comput. Vis. Pattern Recog. Worksh.*, pages 51–59, 2017. 6
- [18] Rajeev Ranjan, Carlos D Castillo, and Rama Chellappa. L2-constrained softmax loss for discriminative face verification. *arXiv preprint arXiv:1703.09507*, 2017. 1, 2, 3
- [19] Ergys Ristani and Carlo Tomasi. Features for multi-target multi-camera tracking and re-identification. In *IEEE Conf. Comput. Vis. Pattern Recog.*, June 2018. 3
- [20] Florian Schroff, Dmitry Kalenichenko, and James Philbin. Facenet: A unified embedding for face recognition and clustering. In *IEEE Conf. Comput. Vis. Pattern Recog.*, pages 815–823, 2015. 1, 2
- [21] Soumyadip Sengupta, Jun-Cheng Chen, Carlos Castillo, Vishal M Patel, Rama Chellappa, and David W Jacobs. Frontal to profile face verification in the wild. In *2016 IEEE Winter Conference on Applications of Computer Vision (WACV)*, pages 1–9. IEEE, 2016. 6
- [22] Kihyuk Sohn. Improved deep metric learning with multi-class n-pair loss objective. In *Advances in neural information processing systems*, pages 1857–1865, 2016. 1, 2
- [23] Yifan Sun, Changmao Cheng, Yuhang Zhang, Chi Zhang, Liang Zheng, Zhongdao Wang, and Yichen Wei. Circle loss: A unified perspective of pair similarity optimization. In *IEEE Conf. Comput. Vis. Pattern Recog.*, 2020. 3
- [24] Yifan Sun, Liang Zheng, Yi Yang, Qi Tian, and Shengjin Wang. Beyond part models: Person retrieval with refined part pooling (and a strong convolutional baseline). In *Eur. Conf. Comput. Vis.*, 2018. 2
- [25] Feng Wang, Weiyang Liu, Haijun Liu, and Jian Cheng. Additive margin softmax for face verification. *arXiv:1801.05599*, 2018. 3
- [26] Feng Wang, Xiang Xiang, Jian Cheng, and Alan Loddon Yuille. Normface: L2 hypersphere embedding for face verification. In *ACM Int. Conf. Multimedia*, pages 1041–1049, 2017. 1, 2, 3
- [27] Hao Wang, Yitong Wang, Zheng Zhou, Xing Ji, Dihong Gong, Jingchao Zhou, Zhifeng Li, and Wei Liu. CosFace: Large margin cosine loss for deep face recognition. In *IEEE Conf. Comput. Vis. Pattern Recog.*, pages 5265–5274, 2018. 1, 2, 3, 7, 8
- [28] Jian Wang, Feng Zhou, Shilei Wen, Xiao Liu, and Yuanqing Lin. Deep metric learning with angular loss. In *Int. Conf. Comput. Vis.*, pages 2593–2601, 2017. 2
- [29] Xiaobo Wang, Shuo Wang, Jun Wang, Hailin Shi, and Tao Mei. Co-mining: Deep face recognition with noisy labels. In *Int. Conf. Comput. Vis.*, pages 9358–9367, 2019. 1, 3

- [30] Yandong Wen, Kaipeng Zhang, Zhifeng Li, and Yu Qiao. A discriminative feature learning approach for deep face recognition. In *Eur. Conf. Comput. Vis.*, pages 499–515. Springer, 2016. [2](#)
- [31] Cameron Whitelam, Emma Taborsky, Austin Blanton, Brianna Maze, Jocelyn Adams, Tim Miller, Nathan Kalka, Anil K Jain, James A Duncan, Kristen Allen, et al. Iarpa janus benchmark-b face dataset. In *IEEE Conf. Comput. Vis. Pattern Recog. Worksh.*, pages 90–98, 2017. [6](#)
- [32] Xiang Wu, Ran He, Zhenan Sun, and Tieniu Tan. A light cnn for deep face representation with noisy labels. *IEEE Transactions on Information Forensics and Security*, 13(11):2884–2896, 2018. [1](#), [3](#)
- [33] Xiaqing Xu, Qiang Meng, Yunxiao Qin, Jianzhu Guo, Chenxu Zhao, Feng Zhou, and Zhen Lei. Searching for alignment in face recognition. In *AAAI*, volume 35, pages 3065–3073, 2021. [2](#)
- [34] Liang Zheng, Liyue Shen, Lu Tian, Shengjin Wang, Jingdong Wang, and Qi Tian. Scalable person re-identification: A benchmark. In *Int. Conf. Comput. Vis.*, 2015. [8](#)
- [35] Yaoyao Zhong, Weihong Deng, Mei Wang, Jiani Hu, Jianteng Peng, Xunqiang Tao, and Yaohai Huang. Unequal-training for deep face recognition with long-tailed noisy data. In *IEEE Conf. Comput. Vis. Pattern Recog.*, pages 7812–7821, 2019. [1](#), [3](#)
- [36] Zhun Zhong, Liang Zheng, Guoliang Kang, Shaozi Li, and Yi Yang. Random erasing data augmentation. In *AAAI*, 2020. [8](#)